

# STRUCTURAL AND CRYSTALLIZATION CHARACTERISTICS OF $K_2O \cdot TiO_2 \cdot 3GeO_2$ GLASS

SNEZANA GRUJIC, NIKOLA BLAGOJEVIC, MIHAJLO TOSIC\*, VLADIMIR ZIVANOVIC\*

*Faculty of Technology and Metallurgy, University of Belgrade,  
Karnegijeva 4, 110 00 Belgrade, Serbia and Montenegro*

*\*Institute for the Technology of Nuclear and Other Mineral Raw Materials,  
Franchet d'Esperey 86, 110 00 Belgrade, Serbia and Montenegro*

E-mail: grujic@tmf.bg.ac.yu

Submitted June 16; accepted September 13, 2005

**Keywords:** Germanate glass, Alkali germanate glasses, Crystallization mechanism

*Structure and crystallization of  $K_2O \cdot TiO_2 \cdot 3GeO_2$  glass have been investigated by means of Fourier transform infrared spectroscopy (FTIR), differential thermal analysis (DTA), differential scanning calorimetry (DSC), x-ray diffraction analysis (XRD), and scanning electron microscopy (SEM). XRD analysis of crystallized glass reveals the presence of crystalline  $K_2O \cdot TiO_2 \cdot 3GeO_2$  indicating the same composition of crystalline and parent glass. For glass particle size  $> 0.15 \mu m$  volume crystallization is dominant crystallization mechanism. SEM investigation of the crystallized glass confirmed volume crystallization of spherical nuclei.*

## INTRODUCTION

Germanate glasses are of interest from technological and scientific standpoint. The use of germanate glasses in technological applications, such as optical fibers and infrared-transmitting windows has stimulated extensive investigation of their properties. The present interest in alkali germanate glass stems from the anomalous change in the properties when alkali oxides are introduced. The appearance of extreme in the properties versus composition curve was first observed by Murthy [1], Shelby [2] and Riebliung [3]. This behavior is widely known as the germanate anomaly and is attributed to a change in the coordination of Ge from four-fold to six-fold for a concentration of not more than 20 mol% of alkali oxide.

There have been a large number of studies concerning the properties and structure of binary and ternary germanate glasses [4-9]. The crystallization behavior of these glasses has been extensively studied, while on the other hand, data on the crystallization behavior of glasses from the  $R_2O-TiO_2-GeO_2$  system are limited [10, 11]. For the glasses of  $K_2O-TiO_2-GeO_2$  system Imaoka [12] described the area of vitrification, but an extensive literature search showed that data for crystallization behavior of glasses in this system are missing.

In the present work the  $K_2O \cdot TiO_2 \cdot 3GeO_2$  glass was investigated by Fourier transform infrared spectroscopy (FTIR), differential thermal analysis (DTA), differential scanning calorimetry (DSC), x-ray diffraction analysis

(XRD) and scanning electron microscope (SEM). The purpose of this work is to study structure and crystallization behavior of this glass and to obtain basic data necessary for further investigation of glass crystallization.

## EXPERIMENTAL

The glass was prepared from  $GeO_2$ , electronic grade (Acros organics),  $K_2CO_3$ , reagent grade (Fluka Chemic) and  $TiO_2$ , reagent grade (Fluka Chemic). Homogeneous mixture of appropriate batch materials was melted in uncovered Pt crucibles in an electric oven at 1200°C for one hour. The molten glass was cast on a metal plate and quenched in air. The amorphous nature as well as homogeneity of the quenched melt was ascertained with XRD and SEM.

The structure of the glass was analyzed by Fourier transform infrared spectroscopy (FTIR). FTIR spectrum was recorded in the wave number range from 400-1400  $cm^{-1}$ , using a MB BOMEN HARTMANN spectrometer. A spectral resolution of 4  $cm^{-1}$  was chosen. Glass sample was mixed with KBr (1 wt.% of glass) and pressed into pellet.

In order to find out the glass transition temperature  $T_g$  and the dilatometric softening temperature  $T_s$  of the glass dilatometric measurement was performed on the sample having: diameter 3 mm and length 30 mm, at the heating rate  $\nu = 10^\circ C/min$  in the temperature range

$T = 20$ - $580^\circ\text{C}$ . Prior the measurement the sample was heated at the heating rate  $\nu = 10^\circ\text{C}/\text{min}$  up to  $600^\circ\text{C}$  then cooled up to  $300^\circ\text{C}$  at the cooling rate  $\nu = 1^\circ\text{C}/\text{min}$  and finally left to cool down up to ambient temperature. In the thermal expansion curve, the temperature of the inflection point is taken as glass transition temperature  $T_g$  while the temperature where the sample reaches a maximum length as dilatometric softening temperature  $T_o$  [13].

The peak temperature of crystallization  $T_p$  and melting  $T_m$  as well as crystallization and melting enthalpy of the crystalline phase were determined by a differential scanning calorimetric (DSC) run of glass in a SDT Q600 V7.0 Build 84 instrument at the heating rate  $\nu = 20^\circ\text{C}/\text{min}$ . Temperature and energy calibrations of the instrument were performed using the known melting temperatures and melting enthalpies of high-purity zinc and silver standards.

The pieces of bulk glass were subjected to heat treatment at two temperatures. In the first experiment the bulk glass was heated at the heating rate  $\nu = 10^\circ\text{C}/\text{min}$  up to  $640^\circ\text{C}$  and kept for 1000 min while in the second experiment the bulk glass was heated at the heating rate  $\nu = 10^\circ\text{C}/\text{min}$  up to  $560^\circ\text{C}$  and kept at this temperature for 100 min.

The amorphous nature of glass was confirmed and identification of the crystalline phase formed in bulk glass after heat treatments were carried out by a Philips PW-1710 automated diffractometer.

Determination of the crystallization mechanism of powder glass was carried out by DTA investigations in a STA 409 EP device. For determination of crystallization mechanism powder samples with granulation:  $< 0.037$ ;  $0.037$ - $0.063$ ;  $0.063$ - $0.10$ ;  $0.1$ - $0.2$ ;  $0.2$ - $0.3$ ;  $0.3$ - $0.4$ ;  $0.4$ - $0.5$ ;  $0.5$ - $0.63$ ;  $0.63$ - $0.83$ ;  $0.83$ - $1$  mm were used. The heating rate was  $\nu = 10^\circ\text{C}/\text{min}$  and sample masses were 100 mg. Morphological evidence of proposed crystallization mechanism was collected by scanning electron microscope Jeol JSM T20 on heat treated, platinum sputtered samples.

## RESULTS

The FTIR spectrum of the  $K_2O \cdot TiO_2 \cdot 3GeO_2$  glass recorded in the interval  $400$ - $1400$   $\text{cm}^{-1}$  is shown in figure 1. The spectrum exhibits expected broad absorption bands as the consequence of the general disorder of glassy state. Two absorption regions could be observed, the most intense absorption band, exhibiting a shoulder in the higher wavenumbers region, lies in the  $1000$ - $700$   $\text{cm}^{-1}$  and second absorption region lies between  $650$ - $400$   $\text{cm}^{-1}$ .

Table 1 shows the characteristic temperatures of the  $K_2O \cdot TiO_2 \cdot 3GeO_2$  glass. Glass transition  $T_g$  and dilatometric  $T_o$  temperatures are determined from thermal

expansion curve, while the peak temperature of crystallization  $T_p$  and of melting  $T_m$  from DSC curve. The values of crystallization  $\Delta H_c$  and melting enthalpy  $\Delta H_m$ , determined from DSC curve, are given in table 1 too.

The DSC curve of the  $K_2O \cdot TiO_2 \cdot 3GeO_2$  glass is shown in figure 2. The XRD pattern of glass heated at  $T = 640^\circ\text{C}$  for  $t = 1000$  min (figure 3) shows several sharp diffractions that were assigned to crystalline  $K_2O \cdot TiO_2 \cdot 3GeO_2$ .

Table 1. Characteristic temperatures, crystallization and melting enthalpy of the  $K_2O \cdot TiO_2 \cdot 3GeO_2$  glass determined by dilatometric and DSC measurements.

	$T_g$ ( $^\circ\text{C}$ )	$T_o$ ( $^\circ\text{C}$ )	$T_p$ ( $^\circ\text{C}$ )	$T_m$ ( $^\circ\text{C}$ )	$\Delta H_c$ (kJ/mol)	$\Delta H_m$ (kJ/mol)
Dilatometr.	550	575	-	-	-	-
DSC	550	573	648	1035	92.8	134.7

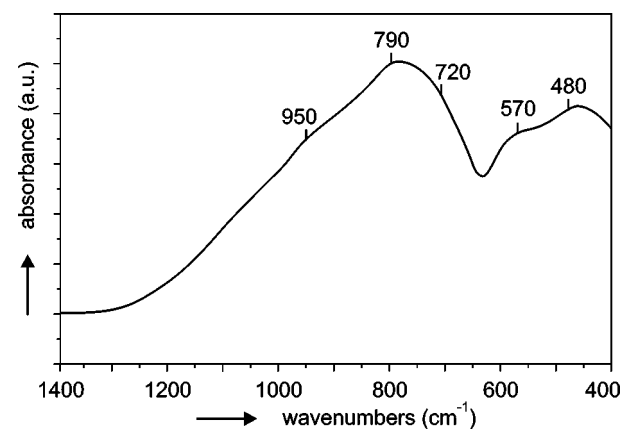


Figure 1. FTIR spectrum of the  $K_2O \cdot TiO_2 \cdot 3GeO_2$  glass.

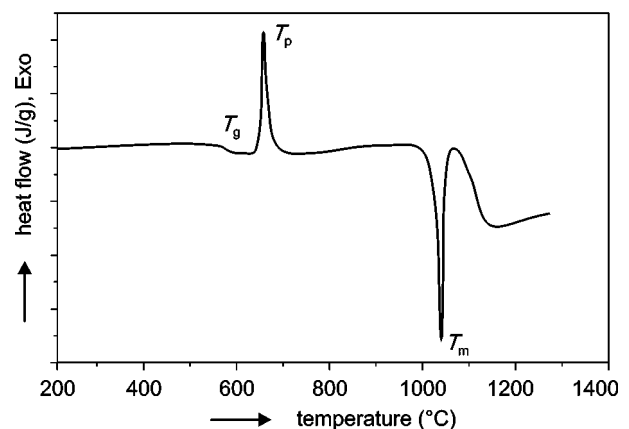


Figure 2. The DSC curve recorded at the heating rate  $\nu = 10^\circ\text{C}/\text{min}$  for the sample with the mean particle size  $0.565$  mm.

The values of characteristic temperatures ( $T$ ) and corresponding viscosities ( $\eta$ ) were fitted using the Vogel-Fulcher-Tamann equation (VFT) giving:

$$\log \eta = -0.286 + \frac{1739.14}{T - 683.88} \quad (1)$$

where  $\eta$  is given in Pa s and  $T$  is the absolute temperature.

The viscosity versus temperature plot is given in figure 4, together with the  $\log \eta$  versus  $1/T$  plot (inset). From the line slope of  $\log \eta$  versus  $1/T$  activation energy for viscous flow  $E_\eta$  was estimated to be 959 kJ/mol.

To evaluate the influence of surface area on the crystallization mechanism, DTA curves of glass fractions with granulation: < 0.037; 0.037-0.063; 0.063-0.10; 0.1-0.2; 0.2-0.3; 0.3-0.4; 0.4-0.5; 0.5-0.63; 0.63-0.83; 0.83-1 mm were recorded. From DTA

curves, the peak temperature of crystallization  $T_p$ , the width at half-peak maximum height (peak width)  $(\Delta T)_p$  and maximum height of DTA peak  $(\delta T)_p$  were determined. Figure 5a presents the dependence of the peak temperature of crystallization  $T_p$  on the mean value of the glass particles size while figure 5b shows the influence of particle size on peak width  $(\Delta T)_p$ .

The SEM micrograph of the sample heated at  $T = 560^\circ\text{C}$  for 100 min is shown in figure 7.

### DISCUSSION

The highest absorption band in figure 1 on FTIR spectrum of the  $\text{K}_2\text{O TiO}_2 3\text{GeO}_2$  is at  $790 \text{ cm}^{-1}$ . From previous studies it is known that in the infrared spectrum of  $\text{GeO}_2$ , in which the coordination number of ger-

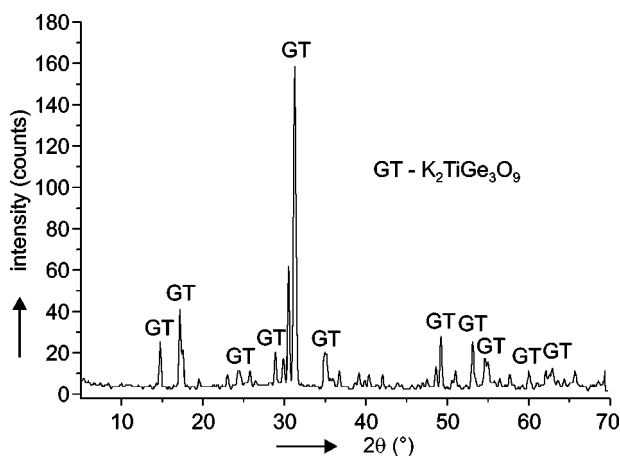


Figure 3. The XRD pattern of the glass crystallized at the  $T = 640^\circ\text{C}$  for  $t = 1000$  min.

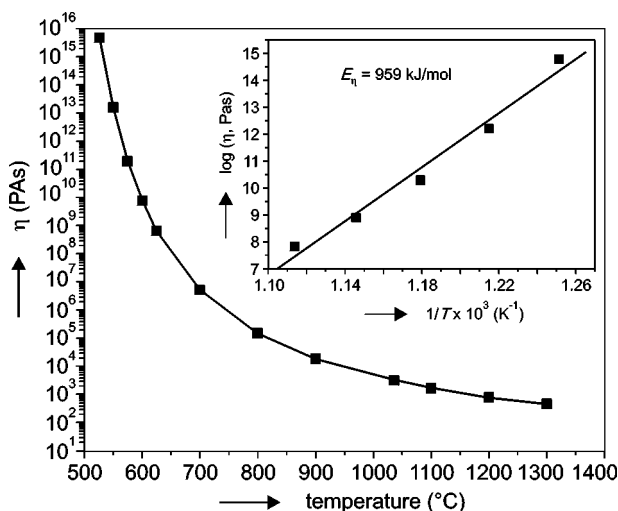
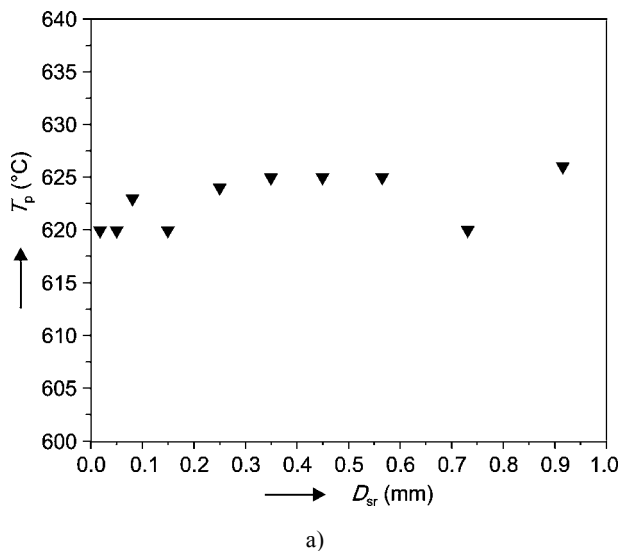
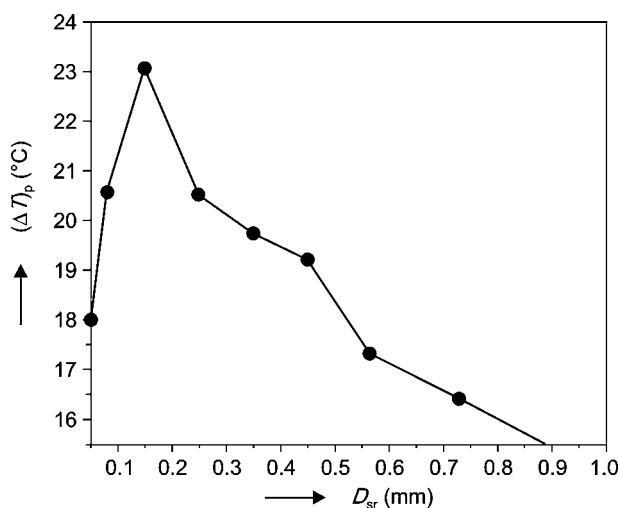


Figure 4. The temperature dependence of the viscosity. Inset:  $\log \eta$  versus reciprocal temperature of the  $\text{K}_2\text{O} \cdot \text{TiO}_2 \cdot 3\text{GeO}_2$ .



a)



b)

Figure 5. a) Dependence of the  $T_p$  on the mean value of the glass particles size. b) Dependence of the  $(\Delta T)_p$  on the mean value of the glass particles size.

manium is four, the absorption band at ca.  $915\text{ cm}^{-1}$  appears due to Ge–O–Ge stretching [14]. In alkali germanate glass the maximum of the absorption band belonging to Ge–O–Ge stretching is shifted to lower wave number [14]. This shift can be related to a change in coordination number from four to six. The higher the number of six coordinated germanium the greater is the shift. In the FTIR spectrum of potassium tetragermanate glass [14-15] the maximum of absorption band lies at ca.  $790\text{ cm}^{-1}$  just like in our investigated glass. This result suggests that molar ratio  $GeO_6/GeO_4$  did not change by introduction of  $TiO_2$ . The band at about  $720\text{ cm}^{-1}$  is related to Ti–O stretching of  $TiO_4$  structural units. The second strong region of absorption may be related to mixed stretching-bending motions:  $570\text{--}480\text{ cm}^{-1}$  stretching vibrations of a  $TiO_6$  [16] and bending vibration of O–Ge–O at about  $560\text{ cm}^{-1}$  [17].

Characteristic temperatures obtained from dilatometric and DSC measurement (figure 2) were used to calculate Hruby parameter [18], a quick measure of glass stability towards crystallization upon reheating, which is given by :

$$K_{gl} = \frac{T_p - T_g}{T_m - T_p} \quad (2)$$

The larger the  $K_{gl}$  the greater is the stability of glass against crystallization. Hruby parameter of the investigated glass is 0.253 indicating not high stability against crystallization.

The degree of fragility  $m$  of the glass melt was evaluated using equation (3),

$$m = \frac{d(\log\eta)}{d(T_g/T)} = \frac{E_\eta}{2.303 RT_g} \quad (3)$$

where  $E_\eta$  is the activation energy for viscous flow.

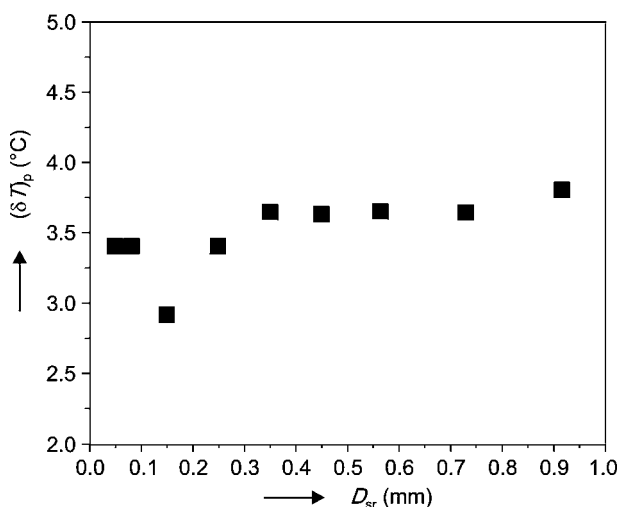


Figure 6.  $(\delta T)_p$  vs. particle size.

Obtained value  $m = 60$  indicates fragile character of the investigated glass. This value is much greater than those for silicate, borate and germania glass melts.

It is obvious from figure 5a that  $T_p$  shows no dependence on the particle size, meaning that glass resistance to crystallization is not influenced by the size of glass particles.

The shape of DTA peak is strongly affected by the crystallization mechanism. Sharp and broad peaks correspond to bulk and surface mechanism, respectively [19-23].

Peak width  $(\Delta T)_p$  increases with increasing particle size up to  $\sim 0.15\text{ mm}$  and then decreases as the particle size increases (figure 5b). In the particle size range up to  $0.15\text{ mm}$  the crystallization peaks are broad (higher peak width) and become sharper (smaller peak width) for the glass particles size  $> 0.15\text{ mm}$ . This means that with increasing particle size broad peaks, corresponding to surface crystallization, change into sharp peaks, characteristic of the volume crystallization.

C. Ray et al [19] developed method that identifies dominant crystallization mechanism by plotting maximum height of the DTA crystallization peak,  $(\delta T)_p$ , as the function of particle size.

Value of the  $(\delta T)_p$  is proportional to the total number of nuclei (surface and volume combined) present in the glass. The ratio of the volume to the total effective area of glass particle size increases with increasing particle size for fixed amount of sample. When surface crystallization is dominant mechanism, total effective area of the glass particles and number of surface nuclei available for crystallization decreases with increasing particle size, and therefore  $(\delta T)_p$  decreases. For dominant volume crystallization an increase in  $(\delta T)_p$  should be observed with increasing particle size, due to increase of number of volume nuclei.

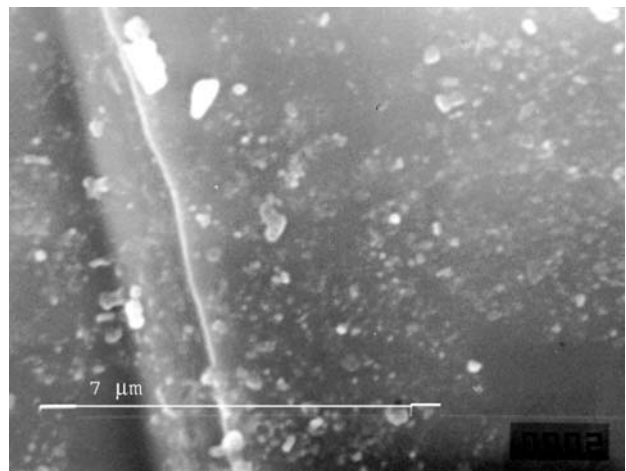


Figure 7. SEM micrograph of glass crystallized at  $T = 560^\circ\text{C}$  for  $t = 100\text{ min}$ . The bar denotes  $7\text{ }\mu\text{m}$ .

The plot in figure 6 shows a decrease of  $(\delta T)_p$  with increasing particle size up to  $\sim 0.15$  mm and increase for the particle size  $> 0.15$  mm. This result suggests a tendency for surface crystallization when particle size is  $< 0.15$  mm that changes to volume crystallization when particle size exceeds  $\sim 0.15$  mm.

The presence of volume crystallization in the SEM micrograph (figure 7) of the bulk glass sample crystallized at  $560^\circ\text{C}$  for 100 min is consistent with proposed crystallization mechanism according to the DTA results.

## CONCLUSIONS

Investigations of structure and devitrification behavior of  $\text{K}_2\text{O}\cdot\text{TiO}_2\cdot 3\text{GeO}_2$  have shown the following:

- The FTIR spectrum of glass indicates presence of  $[\text{GeO}_4]$  and  $[\text{GeO}_6]$  structural units and four-fold and six-fold coordination of Ti.
- XRD analysis of glass crystallized at  $T = 640^\circ\text{C}$  for  $t = 1000$  min approved the presence of crystalline  $\text{K}_2\text{O}\cdot\text{TiO}_2\cdot 3\text{GeO}_2$  indicating polymorphic crystallization (composition of the crystalline phase and parent glass are the same).
- The glass transition temperature, dilatometric softening temperature, the peak temperature of crystallization and melting temperature are  $550^\circ\text{C}$ ,  $575^\circ\text{C}$ ,  $640^\circ\text{C}$  and  $1035^\circ\text{C}$ , respectively. The crystallization enthalpy of crystalline  $\text{K}_2\text{O}\cdot\text{TiO}_2\cdot 3\text{GeO}_2$  is  $92.8$  kJ/mol and melting enthalpy is  $134.7$  kJ/mol, as determined by DSC.
- The degree of fragility  $m$  estimated from activation energy for viscous flow and glass transition temperature is  $m = 60$  indicating a fragile character of  $\text{K}_2\text{O}\cdot\text{TiO}_2\cdot 3\text{GeO}_2$  glass melt.
- The crystallization mechanism depends on particle size. The critical particle size above which the crystallization mechanism changes from surface to volume has been found to be  $\sim 0.15$  mm.
- Microstructure investigation of bulk glass crystallized at  $560^\circ\text{C}$  for 100 min confirmed volume crystallization of spherical nuclei.

## References

1. Murthy M. K. Kirby E. M.: *Phys.Chem.Glasses* 5, 144 (1964).
2. Shelby J.E.: *J.Am.Ceram. Soc* 57, 436 (1974).
3. Riebling E. F.: *J.Chem.Phys.* 39, 1889 (1963).
4. Laudisio G., Catauro M., Luciani G.: *Mater.Chem. Phys.* 58, 109 (1999).
5. Furukawa T., White W.: *J.Mater.Sci.* 15, 1648 (1980).
6. Catauro M., Laudisio G., Marotta A.: *J.Mater.Sci.Lett* 19, 783 (2000).
7. Pernice P., Aronne A., Catauro M., Marotta A.: *J.Non-Cryst.Solids* 210, 23 (1997).

8. Salmam S. M., Salama S. N., Darwish H.: *Ceramics - Silikáty* 47, 63 (2003).
9. Aronne A., Catauro M., Pernice P.: *Thermochim.Acta* 259, 269 (1995).
10. Aronne A., Catauro M., Pernice P., Marotta A.: *Mater. Chem.Phys.* 34, 86 (1993).
11. Laudisio G., Catauro M.: *Thermochim.Acta* 320, 155 (1998).
12. Margaryan A., Piliavin M.: *Germanate Glasses: Structure, Spectroscopy, and Properties*, p. 26-33, Artech House, Boston, London 1993.
13. Shelby J. E.: *Introduction to Glass Science and Technology*, p.111, The Royal Society of Chemistry, Cambridge, United Kingdom, 1997.
14. Yiannopoulos Y. D., Kamitsos E. I., Jain H. in: *Physics and Applications of Non-Crystalline Semiconductors in Optoelectronics*, p.317-325, Ed. Andriesh A., Bertolotti M. Kluwer Academic Publisher, Amsterdam 1997.
15. Laudisio G., Catauro M.: *J.Thermal.Anal.* 52, 967 (1998).
16. Shaim A.: *Materials Research Bulletin* 37, 2459 (2002).
17. Blaszczyk K., Adamczyk M., Wedzikowska M., Rokita M.: *J.Mol.Struct.* 704, 275 (2004).
18. Hruby A.: *Czech J.Phys B* 22, 1187 (1972).
19. Ray C. S., Yang Q., Huang H., Day D. E.: *J.Am.Ceram. Soc.* 79, 3155 (1996).
20. Marotta A., Buri A., Branda F.: *J.Thermal.Anal.* 21, 227 (1981).
21. Marotta A., Buri A.: *Thermochim.Acta* 40, 397 (1980).
22. Marotta A., Buri A., Branda F.: *J.Mater.Sci.* 16, 341 (1981).
23. Xu X.J., Ray C.S., Day D.E.: *J.Am.Ceram.Soc.* 74, 909 (1991).

## STRUKTURNÍ A KRYSTALIZAČNÍ CHARAKTERISTIKY $\text{K}_2\text{O}\cdot\text{TiO}_2\cdot 3\text{GeO}_2$ SKEL

SNEZANA GRUJIC, NIKOLA BLAGOJEVIC, MIHAJLO TOSIC\*, VLADIMIR ZIVANOVIC\*

*Faculty of Technology and Metallurgy,  
University of Belgrade,  
Karnegijeva 4, 11000 Belgrade, Serbia and Montenegro  
\*Institute for the Technology of Nuclear  
and Other Mineral Raw Materials,  
Franchet d'Esperey 86, 11000 Belgrade,  
Serbia and Montenegro*

Struktura a vlastnosti  $\text{K}_2\text{O}\cdot\text{TiO}_2\cdot 3\text{GeO}_2$  skel byly zkoumány infračervenou spektrometrií s Fourierovou transformací (FTIR), diferenční termickou analýzou (DTA), diferenční skenovací kalorimetrií (DSC), RTG difrakční analýzou (XRD) a skenovací elektronovou mikroskopií (SEM). RTG analýza zkrytalovaných skel odhalila přítomnost krystalického  $\text{K}_2\text{O}\cdot\text{TiO}_2\cdot 3\text{GeO}_2$  ukazující totožné složení krystalické a skelné fáze. Dominujícím mechanismem krystalizace částic skla větších než  $0,15$  mm je objemová krystalizace sférických nukleí, která byla rovněž potvrzena SEM analýzou.